Available online at www.sciencedirect.com
SCIENCE DIRECT®
J. of Supercritical Fluids 29 (2004) 69–75
THE JOURNAL OF Supercritical Fluids
www.elsevier.com/locate/supflu

Double retrograde vaporization in a multi-component system: ethane + orange peel oil

S. Raeissi, C.J. Peters*

Laboratory of Applied Thermodynamics and Phase Equilibria, Faculty of Applied Sciences, Delft University of Technology, Julianalaan 136, 2628 BL Delft, The Netherlands

Received 11 October 2002; received in revised form 14 March 2003; accepted 17 March 2003

Abstract

Among the various peculiar infinite-dilute near-critical phase behavior phenomena, one can mention "double retrograde vaporization" (DRV). This phenomenon is characterized by displaying two "domes" on the retrograde dew point curve, instead of the single-domed dew point curve in the familiar "single" retrograde condensation. This behavior had previously been observed in binary systems. This study shows that DRV also occurs in systems composed of a larger number of components. This is in line with a previous suggestion that the phenomenon of DRV is general. Experiments were carried out on the multi-component system ethane + orange peel oil, indicating quadruple-valued dew points at certain concentrations. Bubble point, dew point and critical point temperatures and pressures are presented for five different compositions ranging from 97.8 to 99.9 mass percent ethane. The data range within temperatures and pressures of 285–363 K and 3–7 MPa, respectively. The shapes and trends of DRV of the multi-component system ethane + orange peel oil are compared with those of the binary system ethane + limonene.

Keywords: Phase behavior; Liquid–vapor equilibria; Retrograde condensation; Dew point; Citrus oil; Essential oil

1. Introduction

Recent decades have witnessed a significant amount of research activity focusing on the application of supercritical fluids in the process industry. Many of these applications, such as supercritical extraction, involve solutions having very dilute concentrations of the solute. An important requirement in such developments is knowledge of the thermodynamic properties of these systems. In the near-critical region, the correct understanding of such properties is of particular significance as they can assume highly nonlinear behavior for very dilute mixtures, for example, a strong divergence in the partial molar volume of the solute, a curious concentration dependence of the excess enthalpy, large negative values of apparent molar heat capacities, steep increases in supercritical solubility, and path dependence of thermodynamic derivatives such as the partial molar volume [1].

Among the various interesting infinite-dilute near-critical phenomena, one can point out to the peculiar S-shaped or double-domed dew point behavior, referred to as double retrograde vaporization (DRV) [2]. This phenomenon was noticed experimentally

* Corresponding author. Tel.: + 31-15-278-2660; fax: + 31-15-278-8047
E-mail address: cor.peters@tnw.tudelft.nl (C.J. Peters).

0896-8446/$ – see front matter © 2003 Elsevier B.V. All rights reserved.
doi:10.1016/S0896-8446(03)00068-8

Nomenclature

A	more volatile component
G	gas
L	liquid
P	pressure
T	temperature

by Chen et al. [3] for the system methane + butane. Further experimental evidence of DRV followed in the studies of Chen et al. [4], Chu et al. [5], and Kahre [6] for methane + pentane, of Bischoff and Rosenbauer [7] for water + sodium chloride, and of Raeissi and Peters [8,9] for ethane + limonene and ethane + linalool. Certain studies dedicated to simulating this behavior [2,10–13], indicated the ability of even simple equations of state in qualitatively predicting the phenomenon and (semi) quantitatively reproducing the data. This further validates the phenomenon from a fundamental point of view. In addition to the theoretical importance of DRV as a phase behavior phenomenon, helping in the better understanding of the fundamentals of infinite-dilute near-critical behavior, DRV may also open up new opportunities for applications. One such study [14] suggests the use of the extreme solubility peaks characteristic of DRV, to increase the efficiency of supercritical fluid extraction.

As part of a general study to investigate the superiority of supercritical ethane over supercritical carbon dioxide in deterpenating citrus essential oils, this study is dedicated to the experimental determination of DRV in the multi-component system ethane + orange peel oil. Orange peel oil is obtained from small glands in the colored portion of the peel of the fruit. It is composed of numerous compounds including unsaturated terpenes and sesquiterpenes, and oxygenated compounds such as aldehydes, alcohols, ketones, esters, ethers, and phenols. However, the major constituent of orange oil by far is the terpene, d-limonene (> 90%). In this respect, the experimental DRV results of ethane + orange oil have also been compared with those of the binary system ethane + limonene.

2. The phenomenon of DRV

It is believed that all mixtures with a high degree of asymmetry (difference in size, shape and/or energy between the solute and solvent molecules) will exhibit the phenomenon of DRV. Instead of the usual double-dew points in the familiar single-retrograde condensation, DRV is characterized by an S-shaped or double-domed retrograde dew point curve in the P-x-y diagram. This results in triple- or quadruple-valued dew points for a single composition. DRV occurs within a very limited composition and temperature range, very close to the critical point of the more volatile component. It is the result of the continuous phase transition from the critical point of the mixture very highly concentrated with the more volatile component to the critical point of pure volatile component (component A). As the concentration of component A progressively increases, the single-domed pressure–temperature phase envelope gradually forms a dent, which progresses to form two distinct domes. We shall name these two domes the “critical dome” and “ non-critical dome” based on their vicinity to the critical point. As the composition of A increases, the “critical dome” gains more and more significance, increasing its temperature boundary, while the “non-critical dome” reduces in size. When compositions approach the limit of pure A, the bubble and dew point curves are forced to approach one another such that it is likely that the “non-critical dome” completely disappears by dissolving into the “critical dome”. Upon reaching 100% pure A, the bubble and dew point curves meet to form a single line, the saturated vapor pressure curve of pure A. Detailed explanations of this phenomenon and the transitions involved are given elsewhere [8,9].

3. Experimental

The Cailletet apparatus used for performing the phase equilibrium experiments operates according to the synthetic method. At any desired temperature, the pressure is varied for a sample of constant overall composition until a phase change is observed visually. Detailed explanations of the apparatus and experimental procedure are given elsewhere [15–17].

Cold-pressed and de-waxed Brazilian orange oil was purchased from Sigma Aldrich, and ethane (99.95 vol.%) was purchased from Messer Griesheim. Both products were used without further purification.

Table 1
Experimental bubble point, dew point, and critical point temperature and pressure data for mixtures of ethane + orange peel oil at five different mass concentrations

99.9% ethane		99.7% ethane		99.6% ethane		99.0% ethane		97.8% ethane	
T (K)	*P* (Mpa)	*T* (K)	*P* (MPa)	*T* (K)	*P* (MPa)	*T* (K)	*P* (MPa)	*T* (K)	*P* (MPa)
Critical point		Critical point		Critical point		Critical point		Critical point	
305.52	4.91	306.31	4.96	306.75	4.99	307.01	5.00	310.43	5.24
LG→G		LG→G		LG→G		LG→G		LG→G	
305.55	4.91	Upper branch		306.76	4.99	307.01	5.00	310.59	5.25
G→LG		306.32	4.96	306.81	4.99	307.07	5.00	310.59	5.25
293.70	3.63	306.33	4.96	306.84	4.99	307.18	5.01	310.77	5.26
293.98	3.67	306.38	4.96	307.07	5.01	307.20	5.01	313.11	5.41
294.30	3.70	306.48	4.97	307.27	5.01	307.42	5.02	313.25	5.43
294.91	3.77	306.54	4.97	307.35	5.02	307.62	5.03	318.06	5.66
295.14	3.79	306.61	4.97	307.38	5.02	307.82	5.04	322.97	6.05
295.31	3.81	306.62	4.97	307.40	5.01	307.89	5.04	327.91	6.15
295.48	3.83	306.66	4.97	307.43	5.01	307.95	5.03	332.88	6.38
296.00	3.88	306.66	4.97	307.44	5.01	307.97	5.03	337.87	6.63
296.37	3.93	306.67	4.97	307.46	5.01	308.06	5.02	342.78	6.80
296.89	3.98	306.67	4.95	307.48	5.01	308.12	5.01	347.69	6.95
297.07	3.99	Lower branch		307.50	5.01	308.20	5.00	352.61	7.10
297.51	4.05	305.14	4.52	307.53	5.01	308.23	4.97	357.50	7.25
297.85	4.08	305.25	4.49	307.55	5.00	308.26	4.96	362.56	7.38
298.21	4.12	305.31	4.47	307.56	5.00	308.30	4.96	LG→L	
298.47	4.14	305.51	4.47	307.58	4.99	308.51	4.92	288.42	3.40
298.89	4.18	305.63	4.45	307.60	4.99	308.68	4.90	293.28	3.77
299.21	4.22	305.80	4.42	307.61	4.97	308.85	4.89	298.23	4.18
299.54	4.25	305.90	4.41	307.62	4.92	309.02	4.87	303.20	4.61
299.94	4.30	306.18	4.40	307.63	4.92	309.24	4.86	308.13	5.06
300.33	4.34	306.38	4.40	307.66	4.90	309.70	4.83	309.14	5.14
300.55	4.36	306.76	4.37	307.68	4.89	310.24	4.82	310.10	5.21
301.04	4.41	307.08	4.35	307.82	4.83	312.18	4.77	310.31	5.23
301.37	4.45	307.37	4.38	307.83	4.83	314.06	4.74		
302.08	4.52	307.70	4.36	307.85	4.83	316.04	4.73		
302.45	4.56	308.57	4.38	307.87	4.82	318.11	4.69		
302.73	4.60	308.86	4.40	307.95	4.81	321.26	4.64		
303.21	4.65	309.00	4.39	308.01	4.80	324.12	4.56		
303.49	4.67	309.35	4.37	308.06	4.80	326.92	4.46		
303.59	4.68	309.61	4.32	308.14	4.79	LG→L			
303.91	4.72	310.07	4.36	308.32	4.77	288.53	3.42		
304.11	4.74	310.21	4.31	308.37	4.77	293.31	3.79		
304.32	4.78	310.61	4.34	308.37	4.76	298.24	4.20		
304.73	4.81	310.83	4.31	308.52	4.76	303.22	4.65		
304.88	4.82	311.21	4.29	308.63	4.75	304.21	4.75		
305.12	4.85	311.65	4.29	308.91	4.74	305.26	4.85		
305.24	4.87	312.42	4.21	309.17	4.72	306.26	4.94		
305.34	4.88	313.02	4.19	309.57	4.71	306.67	4.98		
305.52	4.91	313.25	4.22	309.84	4.70	306.80	4.98		
LG→L		G→LG		310.31	4.70	306.89	4.99		
293.82	3.85	305.14	4.55	310.86	4.69	306.96	4.99		
295.30	3.97	305.17	4.58	LG→L		306.97	5.00		
296.39	4.07	305.25	4.61	295.04	3.94	306.98	4.99		
297.57	4.17	305.40	4.66	299.44	4.32	306.99	4.99		
298.51	4.25	305.50	4.70	303.25	4.67	307.00	5.00		
299.03	4.30	305.64	4.73	306.08	4.93				
300.48	4.43	306.03	4.81	306.54	4.97				

Table 1 (*Continued*)

99.9% ethane		99.7% ethane		99.6% ethane		99.0% ethane		97.8% ethane	
T (K)	*P* (Mpa)	*T* (K)	*P* (MPa)	*T* (K)	*P* (MPa)	*T* (K)	*P* (MPa)	*T* (K)	*P* (MPa)
301.04	4.48	306.15	4.84	306.70	4.98				
301.40	4.52	306.28	4.86	306.73	4.99				
302.45	4.61	306.30	4.87						
302.46	4.61	306.38	4.89						
303.54	4.72	306.42	4.90						
303.77	4.74	306.46	4.90						
304.26	4.79	306.49	4.91						
304.82	4.84	306.54	4.92						
305.26	4.88	306.57	4.93						
305.48	4.90	306.59	4.93						
305.50	4.91	306.62	4.94						
305.51	4.90	306.66	4.95						
		306.67	4.95						
		306.67	4.96						
		LG→L							
		284.77	3.16						
		288.44	3.43						
		293.93	3.86						
		298.67	4.26						
		303.26	4.68						
		305.25	4.87						
		305.64	4.90						
		306.12	4.95						
		306.16	4.95						
		306.31	4.96						

4. Results and discussion

Table 1 presents the experimentally measured bubble point, dew point, and critical point temperatures and pressures for five different mass compositions of the multi-component system ethane + orange peel oil. Since composition errors are rather high in such highly diluted systems, the percentage of possible errors in composition are also presented in Table 2. Considering the values of the possible errors, the lower and upper composition ranges in which each isopleth may fall within are also given in Table 2. The phase behaviors of these five isopleths are shown graphically in Fig. 1. This figure clearly shows the gradual change in the shape of the dew point curves. Due to the technical limitations of the Cailletet apparatus, it was not possible to measure the low-pressure branch of the dew point curve. Therefore, even though a maximum of three dew points highest in pressure are measured and shown here, it is evident that the dew point curve continues by bending back towards lower temperature and pressure. It is seen that at an ethane mass concentration of 97.8%, the dew curve still has its usual single-domed shape. At 99%, a dent is formed

Table 2
Percent error in composition of each isopleth and the possible composition range of each isopleth based on the possible error

Calculated mass fraction	%error = $100\Delta x/x$	Lower composition limit	Upper composition limit
0.978	0.105	0.977	0.979
0.990	0.060	0.989	0.991
0.996	0.050	0.996	0.997
0.997	0.056	0.997	0.998
0.999	0.050	0.998	0.999

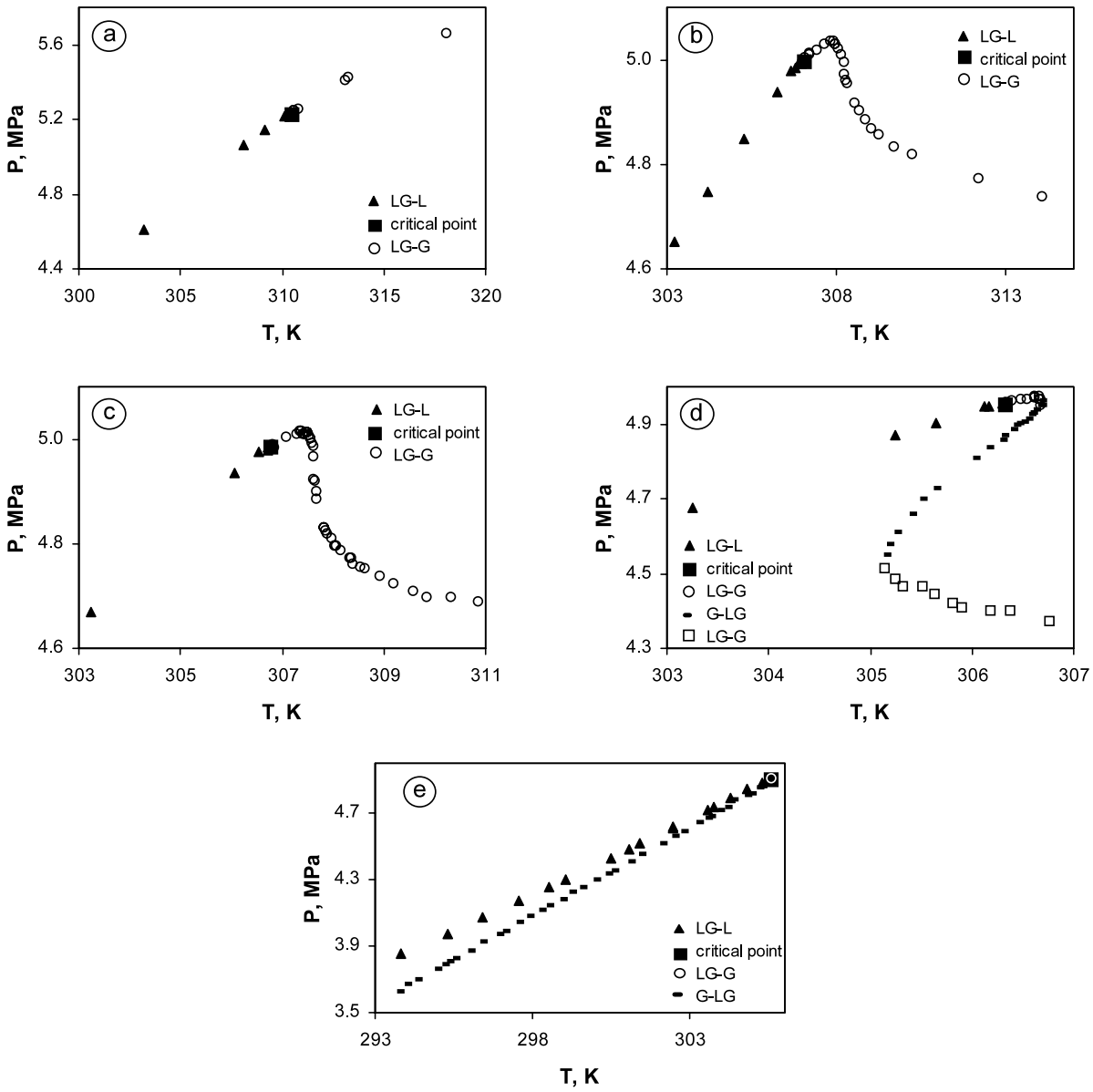

Fig. 1. *P–T* diagrams for five different compositions of the system ethane + orange peel oil. The compositions in mass percent ethane are: (a) 97.8%; (b) 99.0%; (c) 99.6%; (d) 99.7%; (e) 99.9%.

in the dew curve, but not enough to produce multiple dew points. At 99.6%, the dent has progressed further to form an almost vertical slope, indicating the limit that will begin to show quadruple-valued dew points. At 99.7%, DRV has matured enough to produce quadruple dew points. The 99.9% ethane concentration shows only one thin two-phase "critical dome" down to 293.7 K and 3.63 MPa. It is possible that the second "non-critical dome" emerges at still lower temperatures and pressures, or it may be that the upper composition boundary of DRV has already been passed, and hence the single dome continues all the way down to lower pressures and temperatures at the axis of pure orange oil. For comparison, the

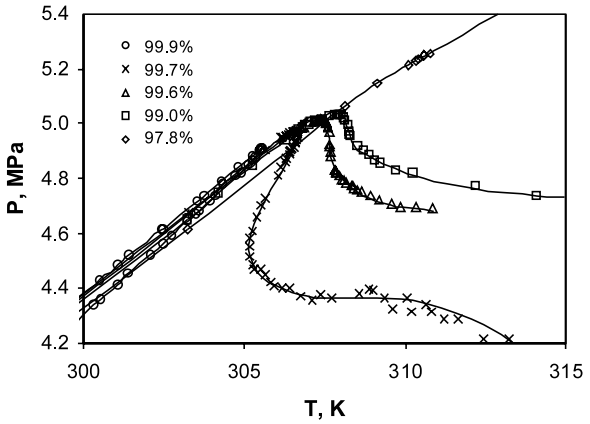

Fig. 2. *P–T* diagrams for the ethane + orange oil isopleths on one scale. All concentrations are given in mass percent ethane.

relative sizes and positions of all five isopleths are shown in Fig. 2 on a single scale.

Fig. 3 compares DRV behavior between ethane+ orange oil to that of ethane and the major constituent of this oil, limonene [8]. The general shapes and trends of DRV in these two systems match so well that it is difficult to distinguish that two different systems have been plotted. However, comparison of the compositions indicates some discrepancies. This may be attributed to the large values of errors in compositions. In fact, the discrepancies of compositions fall within the ranges of error given in Table 2, which are about 0.1 mass percent. For example, the 99% isopleth may

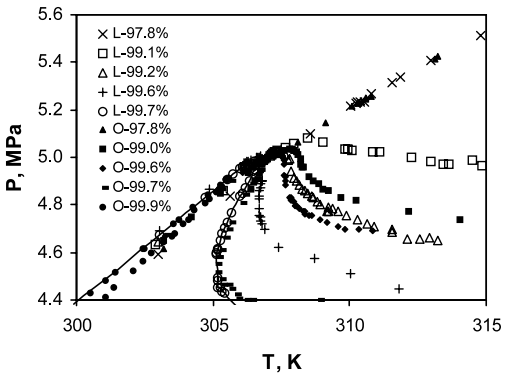

Fig. 3. Comparison of experimental double retrograde behavior between ethane + orange oil and ethane + limonene [8]. The letter "O" in the legend indicates the orange oil system while the letter "L" symbolizes the limonene binary. Concentrations are given in mass percent ethane.

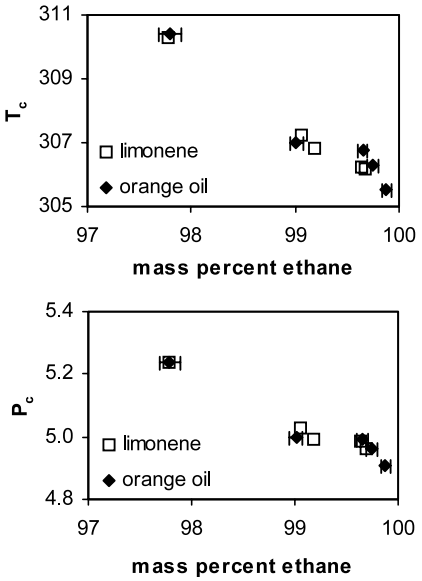

Fig. 4. Experimental mixture critical temperatures and pressures as a function of composition for the systems ethane + orange oil and ethane + limonene [8]. Composition error bars are also shown for ethane + orange oil.

well have a concentration of 99.1% instead. A further comparison is presented in Fig. 4, where the critical temperatures and pressures of these two systems are plotted as functions of ethane concentration. The errors of compositions are more easily seen on these graphs. However, it is still possible to note that the two systems ethane + orange oil and ethane + limonene have very much similar behavior, even though the orange oil is composed of more than 100 components.

5. Conclusion

Experimental vapor–liquid equilibrium data are presented for the system ethane + orange peel oil at very high concentrations of ethane. The results vary within temperature and pressure ranges of 285–363 K and 3–7 MPa, respectively. This system exhibits quadruple-valued dew points characteristic of DRV behavior. The results of this study are compared to those of the binary system ethane + limonene. This comparison shows very similar double retrograde curves and trends between the two systems, regardless of the fact that one is a binary system while the other is composed of numerous components.

References

[1] R.F. Chang, G. Morrison, J.M.H. Levelt Sengers, The critical dilemma of dilute mixtures, J. Phys. Chem. 88 (1984) 3389–3391.

[2] N.F. Carnahan, R.J.J. Chen, D.G. Elliot, P.S. Chappelear, R. Kobayashi, Vapor liquid equilibria in the neighborhood of the critical point in methane–*n*-hydrocarbon systems, in: Presented at IUPAP van der Waals Centennial Conference on Statistical Mechanics, Amsterdam, 1973.

[3] R.J.J. Chen, P.S. Chappelear, R. Kobayashi, Dew point loci for methane–*n*-butane binary system, J. Chem. Eng. Data 19 (1) (1974) 53.

[4] R.J.J. Chen, P.S. Chappelear, R. Kobayashi, Dew point loci for methane–*n*-pentane binary system, J. Chem. Eng. Data 19 (1) (1974) 58.

[5] T.C. Chu, R.J.J. Chen, P.S. Chappelear, R. Kobayashi, Vapor–liquid equilibrium for methane–*n*-pentane system at low temperatures and high pressures, J. Chem. Eng. Data 21 (1) (1976) 41.

[6] L.C. Kahre, Low-temperature *k* data for methane–*n*-butane, J. Chem. Eng. Data 19 (1) (1974) 67.

[7] J.L. Bischoff, R.J. Rosenbauer, The system NaCl–H_2O: relations of vapor–liquid near the critical temperature of water and of vapor–liquid–halite from 300 to 500 °C, Geochem. Cosmochem. Acta 50 (1986) 1437.

[8] S. Raeissi, C.J. Peters, On the phenomena of double retrograde vaporization: multi-dew point behavior in the binary system ethane + limonene, Fluid Phase Equilib. 191 (2001) 33.

[9] S. Raeissi, C.J. Peters, Double retrograde vaporization in the binary system ethane + linalool, J. Supercrit. Fluids 23 (2002) 1.

[10] Y. Arai, R.J.J. Chen, P.S. Chappelear, R. Kobayashi, Prediction of dew point locus in methane–light hydrocarbon binary systems in the neighborhood of the methane critical point, AIChE J. 20 (2) (1974) 399.

[11] S.B. Kiselev, M.Yu. Belyakov, J.C. Rainwater, Crossover Leung-Griffiths model and the phase behavior of binary mixtures with and without chemical reaction, Fluid Phase Equilib. 150–151 (1998) 439.

[12] S. Raeissi, C.J. Peters, Simulation of double retrograde vaporization using the Peng Robinson equation of state, J. Chem. Thermodyn., 35 (2003) 665–673.

[13] S. Raeissi, C.J. Peters, Application of double retrograde vaporization as an optimizing factor in supercritical fluid separation, submitted for publication.

[14] S. Espinosa, S. Raeissi, E.A. Brignole, C.J. Peters, Prediction of the phenomenon of double retrograde vaporization using equations of state, VI Iberoamerican Conference on Phase Equilibria and Fluid Properties for Process Designm, Iguassu Falls, Brazil, Oct. 12–16, 2002.

[15] C.J. Peters, J.L. de Roo, R.N. Lichtenthaler, Measurements and calculations of phase equilibria of binary mixtures of ethane + eicosane. Part I. Vapor + liquid equilibria, Fluid Phase Equilib. 34 (1987) 287.

[16] C.J. Peters, J.L. de Roo, J. de Swaan Arons, Phase equilibria in binary mixtures of propane and hexacontane, Fluid Phase Equilib. 85 (1993) 301.

[17] S. Raeissi, C.J. Peters, Bubble-point pressures of the binary system carbon dioxide + linalool, J. Supercrit. Fluids 20 (2001) 221.